Organic Electronics 10 (2009) 666–673

Contents lists available at ScienceDirect

Organic Electronics

journal homepage: www.elsevier.com/locate/orgel

p-Doped *p*-phenylenediamine-substituted fluorenes for organic electroluminescent devices

Zhi Qiang Gao [a,d,*], Ping Fan Xia [b], Pik Kwan Lo [b], Bao Xiu Mi [a,d,1], Hoi Lam Tam [a,c], Man Shing Wong [a,b,*], Kok Wai Cheah [a,c], Chin H. Chen [e]

[a] Centre for Advanced Luminescence Materials, Hong Kong Baptist University, Kowloon Tong, Hong Kong, SAR China
[b] Department of Chemistry, Hong Kong Baptist University, Kowloon Tong, Hong Kong, SAR China
[c] Department of Physics, Hong Kong Baptist University, Kowloon Tong, Hong Kong, SAR China
[d] Institute of Advanced Materials, Nanjing University of Posts and Telecommunications, Nanjing, China
[e] Display Institute, Microelectronics and Information Systems Research Center, National Chiao Tung University, Hsinchu, Taiwan

ARTICLE INFO

Article history:
Received 22 November 2008
Received in revised form 19 December 2008
Accepted 24 February 2009
Available online 12 March 2009

PACS:
78

Keywords:
Fluorene
p-Phenylenediamine
Hole injection material
Organic electroluminescent devices
Hole transporting materials

ABSTRACT

Two novel *p*-phenylenediamine-substituted fluorenes have been designed and synthesized. Their applications as hole injection materials in organic electroluminescent devices were investigated. These materials show a high glass transition temperature and a good hole-transporting ability. It has been demonstrated that the 2,3,5,6-tetrafluoro-7,7,8,8-tetracyanoquinodimethane (F4-TCNQ) doped *p*-phenylene-diamine-substituted fluorenes, in which F4-TCNQ acts as *p*-type dopant, are highly conducting with a good hole-transporting property. The organic light emitting devices (OLEDs) utilizing these F4-TCNQ-doped materials as a hole injection layer were fabricated and investigated. The pure Alq_3-based OLED device shows a current efficiency of 5.2 cd/A at the current density of 20 mA/cm^2 and the operation lifetime is 1500 h with driving voltage increasing only about 0.7 mV/h. The device performance and stability of this hole injection material meet the benchmarks for the commercial requirements for OLED materials.

© 2009 Elsevier B.V. All rights reserved.

1. Introduction

Organic semiconductors have been intensively studied as active materials in various electronic and optoelectronic devices because of the low cost, ability to tune the functional/material properties by means of chemical structural modifications, ease of fabrication, and feasibility for flexible devices [1]. In addition, the high absorptivity in the visible range of organic semiconductors offers the possibility to prepare a thin-film for photovoltaic cells (OPV) and photodetectors [2]. Hence, in the past decade, these materials have been intensively studied as alternative active materials in various electronic and optoelectronic devices. Recently, enormous progresses have been made in tailoring properties of organic semiconductors through chemical structure modification [3]. Organic semiconductors are generally in the form of undoped amorphous state when used as carrier transporters in thin-film optoelectronic devices. However, the inherent low charge mobility of organic semiconductors resulting from the hopping transport in disordered organic thin-films often gives rise to a high operating voltage. For example, the hole mobility in amorphous organic thin-films is in the range of 10^{-3}–10^{-5} cm^2 v^{-1} s^{-1}, which is about 1000 times lower than that of the amorphous Si thin-film. To improve the

* Corresponding authors. Address: Department of Chemistry, Centre for Advanced Luminescence Materials, Hong Kong Baptist University, Kowloon Tong, Hong Kong, SAR China. Tel.: +852 3411 7069; fax: +852 3411 7348.
E-mail address: mswong@hkbu.edu.hk (M.S. Wong).
[1] Present address: Institute of Advanced Materials, Nanjing University of Posts and Telecommunications, Nanjing, China

1566-1199/$ - see front matter © 2009 Elsevier B.V. All rights reserved.
doi:10.1016/j.orgel.2009.02.025

conductivity of organic semiconductors, doping concepts have been adopted from their inorganic counterparts. Similar to the conventional doping in inorganic semiconductors, the basic concept of doping in organic semiconductor is to add a strong electron-donor or electron-acceptor which either transfer an electron to the lowest unoccupied molecular orbital (LUMO) of a host molecule to produce a free electron (*n*-type doping) or remove an electron from the highest occupied molecular orbital (HOMO) of a host molecule to generate a free hole (*p*-type doping) [4]. In this concept, by matching the LUMO/HOMO of the dopant to the HOMO/LUMO of the organic semiconductor, the Fermi level of the organic semiconductor can be successfully shifted towards the transport states, and hence, the organic devices will be beneficial from reducing ohmic losses, lowering carrier injection barriers and increasing the built-in potential of Schottky- or *p*–*n*-junctions [5]. The organic optoelectronic device with a hole transporting layer (HTL) doped with *p*-type dopant such as 2,3,5,6-tetrafluoro-7,7,8,8-tetracyanoquinodimethane (F4-TCNQ), and an electron transporting layer (ETL) doped with *n*-type dopant such as alkali metal atoms are widely reported, and the device structure is known as *p*–*i*–*n* [6]. Currently, *p*–*i*–*n* organic light emitting devices (OLED) [7] and *p*–*i*–*n* OPV [8] are two of the hot topics in the organic optoelectronic devices due to the improved ohmic contact and electrical conductivity in the devices. For instance, a very low-operation-voltage multilayered OLED with high efficiency has been achieved by combining a thick F4-TCNQ doped 4,4′,4″-*tris*(*N*,*N*-diphenylamino)-triphenylamine (TDATA) as a HTL with a thin undoped buffer layer [9]. This OLED exhibits a turn-on voltage of 2.5 V at a luminance of 1 cd/m^2 and an operating voltage of 3.4 V at a luminance of 100 cd/m^2 for pure *tris*-(8-hydroxyquinoline) aluminum (Alq_3) device without dopant emitter. Most recently, a *p*–*i*–*n* white OLED reached a high efficiency of 23.3 lm/W [10]; and a *p*–*i*–*n* red phosphorescent OLED obtained an external quantum efficiency of 12.4% with extremely high lifetime of about 1×10^7 h [11]. Among the *p*-doped hole transporting systems, F4-TCNQ is the-state-of-art dopant, and most of the host materials for *p*-doping are based on the wide bandgap amorphous hole transporting materials with triphenylamine unit, such as 4,4′,4″-*tris*-*N*-naphthyl-*N*-phenylamino-triphenylamine (TNATA), *N*,*N*,*N*′, *N*′-*tetrakis*-(4-methoxyphenyl)benzidine (MeO-TPD) [7a], 4,4′,4″-*tris*(3-methylphenyl-phenyl-amino)triphenylamine (m-MTDATA) [7b]. Low bandgap metal phthalocyanines can also be efficiently doped with F4-TCNQ. However, phthalocyanines are not well suited for OLEDs due to their small energy gap between HOMO and LUMO levels of phthalocyanines, which leads to re-absorption and electron injection from the emitting layer to the HTL [12]. Other type of materials that can be doped with F4-TCNQ are very rarely reported. In the practical point of view, device stability is an important issue that governs the key factor to realize the success of commercialization. In order to achieve the practically targeted stability, organic semiconductors with high thermal stability are necessary to be developed. Fluorene derivatives have been received considerable attention as potential candidates for the active materials in OLED due to their good chemical stability and high luminescence over the past decade [13]. By attaching appropriate functional substituent, fluorene derivatives can act as a HTL [14], or an ETL [15], or a deep-blue emitting material (EM) [16] in OLEDs. To the best of our knowledge, there is no report on the applications of fluorene derivatives as a *p*-doping host in OLEDs. In this contribution, we have designed and synthesized two new *p*-phenylenediamine-substituted fluorenes for the hole injection application. It is anticipated that these materials show a high glass transition temperature (T_g) and a good hole transport ability because of the highly thermally stable nature of fluorene and phenylenediamine moieties as well as the good hole transporting property of phenylenediamine functional group. We have demonstrated that controlled *p*-type doping system using F4-TCNQ as a dopant can be extended to materials with a fluorene core which was found to be efficient and stable in application of OLED devices. It has been shown that high conductivities can be achieved through doping with F4-TCNQ in these two derivatives. On the other hand, for good device performance, the ionization potential of the host also plays an important role. The lower the ionization potential of the host, the better is the performance. The best Alq_3-based OLED device using such a host material doped with F4-TCNQ as a hole injection layer (HIL) shows an efficiency of 5.2 cd/A and operation lifetime of 1500 h at 20 mA/cm^2, with the driving voltage increasing about 0.7 mV/h. This material with the best performance can be used to replace the currently employed triphenylamine based HIL materials.

2. Results and discussion

2.1. Synthesis and characterization

Scheme 1 shows the synthetic route utilized to prepare *p*-phenylenediamine-substituted fluorenes, **4a** and **4b**. 2,7-dibromofluorene derivatives **1a** and **1b** were prepared according to the literature procedures [16a]. Double amination of 2,7-dibromofluorene derivatives **1a** and **1b** with two equivalent of diphenylamine in the presence of $Pd(OAc)_2$:2P(*o*-tolyl)$_3$ as a catalyst afforded the corresponding diamination product **2a** and **2b** in 72% and 68% yield, respectively. Bromination of diphenylamino end-capped fluorene derivatives **2a** and **2b** with NBS in chloroform yielded tetrabromo-substituted intermediates **3a** and **3b** in excellent yields. Palladium catalyzed amination of **3a** and **3b** with diphenylamine afforded the desired *p*-phenylenediamine-substituted fluorene derivatives in good yields. All the newly synthesized hole injection materials were fully characterized with ^{1}H NMR, ^{13}C NMR, MALDI-TOF HRMS, and elemental analysis and found to be in good agreement with their structures. The detail procedures are shown in experimental section. These fluorene derivatives were purified by the flash column chromatography and degassed under vacuum before used for deposition.

Table 1 summarizes the physical properties measured by the corresponding techniques. As determined by differential scanning calorimeter and thermal gravimetric ana-

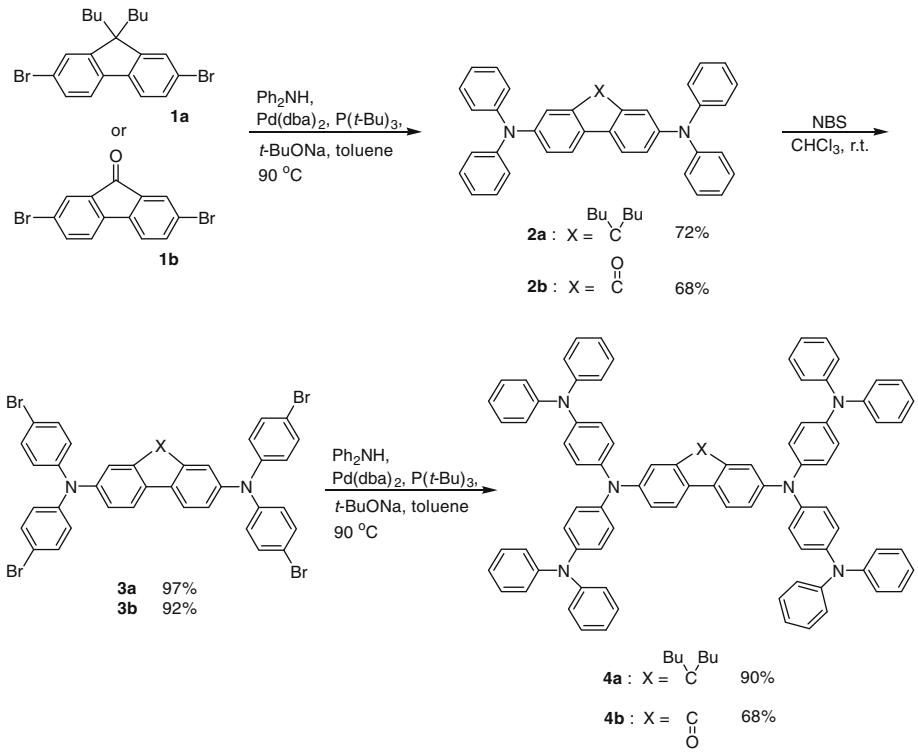

Scheme 1. Synthesis of *p*-phenylenediamine-substituted fluorene derivatives **4a** and **4b**.

Table 1
Summaries of physical measurements of **4a** and **4b**.

	Absorption band/nm[a]	$E^{oxd}_{1/2}$/V[b]	E^{red}_{p}/V[b]	HOMO/eV[c]	LUMO eV[d]	T_g/°C[e]	T_{dec} /°C[f]
4a	309/354/394	0.39, 0.52, 0.86	−1.00	−5.07	−2.16	126	521
4b	314/348/400	0.48, 0.58, 0.89	−1.27	−5.16	−2.34	146	590

[a] Measured in $CHCl_3$.
[b] $E^{oxd}_{1/2}$ (or E^{red}_{p}) vs. SCE estimated by CV method using platinum disc electrode as a working electrode, platinum wire as a counter electrode, and SCE as a reference electrode with an agar salt bridge connecting to the oligomer solution and ferrocene was used as an external standard, $E_{1/2}$ (Fc/Fc^+) = 0.50 V vs. SCE).
[c] Determined by ultraviolet photoemission spectroscopy using Surface Analyzer model AC-2.
[d] LUMO = HOMO − Optical Bandgap.
[e] Determined by differential scanning calorimeter with a heating rate of 10 °C min^{-1} under N_2.
[f] Determined by thermal gravimetric analyzer with a heating rate of 10 °C min^{-1} under N_2.

lyzer with a heating rate of 10 °C min^{-1} under N_2, both fluorene derivatives possess a high glass transition temperature (T_g), > 125 °C and thermal decomposition temperature (T_{dec}), >520 °C, respectively. Such high T_g values are superior to most of the commonly used hole transporting materials (i.e. T_g of 4,4′,4″-*tris*(*N*-(2-naphthyl)-*N*-(phenylamino)triphenylamine (2T-NATA) = 110 °C) [17]. It is well-known that the higher the T_g of a material, the better is the morphological stability of an organic thin-film. Hence, high morphological stability is anticipated using these materials as a hole transporting material in an OLED application.

Cyclic voltammetry (CV) was carried out in a three-electrode cell set-up with 0.1 M of Bu_4NPF_6 as a supporting electrolyte in CH_2Cl_2 to examine the electrochemical properties of these molecules. All the potentials reported are referenced to Fc/Fc^+ standard and the results are tabulated in Table 1. These fluorene derivatives exhibit a low first reversible one-electron anodic redox wave corresponding to phenylenediamine oxidation with $E^{oxd1}_{1/2}$ at 0.39–0.48 V and followed by a reversible one-electron and two-electron anodic redox waves with $E^{oxd2}_{1/2}$ at 0.52–0.58 V and $E^{oxd3}_{1/2}$ at 0.86–0.89 V, respectively. Such a facile first electrochemical oxidation of phenylenediamine moiety suggests a very low first ionization potential of the materials which was confirmed by the estimated HOMO level around −5.1 eV as determined by ultraviolet photoemission spectroscopy. The low HOMO level make them feasible to be removed an electron to generate a free hole upon doped with a strong electron-acceptor. On the other hand, these fluorene derivatives also exhibit an irreversible cathodic wave with $E^{red1}_{1/2}$ at −1.00 to −1.27 eV, which corresponds to the formation of the radical anion on the fluorene/fluorone core.

2.2. Charge-transfer complex of 4 and F4-TCNQ

Due to the strong electron-donating nature of **4** and the strong electron-accepting property of F4-TCNQ, **4** and F4-TCNQ can interact to form a charge-transfer (CT) complex via partial electron transfer upon mixing with which free carriers would be generated as depicted in Fig. 1. There are two possible reaction routes for one-electron transfer between electron-donor **4** and electron-acceptor F4-TCNQ, as shown in Fig. 1. Assuming that there is only one route dominates the one-electron transfer process, the reaction between **4** (represented as D) and F4-TCNQ (represented as A) can be written as [18]:

$$D + A \overset{K}{\rightleftharpoons} D^+ + A^- \quad E_{1A} - E_{1D} \tag{1}$$

where, E_{1A} and E_{1D} are the first reduction potential of the electron-acceptor and the first oxidation potential of the electron-donor, respectively. Thus the equilibrium constant (K) for electron transfer can be given:

$$\log K = \log\left[\frac{[D^+][A^-]}{[D][A]}\right] = \frac{E_{1A} - E_{1D}}{0.059} \tag{2}$$

Using E_{1D} of 0.39 and 0.48 V for **4a** and **4b** from Table 1, respectively and E_{1A} of 0.568 V for F4-TCNQ [19], the reaction constants of $K_{\mathbf{4a}\text{-F4-TCNQ}}$ and $K_{\mathbf{4b}\text{-F4-TCNQ}}$ obtained were $10^{3.02}$ and $10^{1.49}$, respectively. With such large positive values, the corresponding reactions for one-electron transfer between **4** and F4-TCNQ are likely to occur. The occurrence of such electron transfer reactions are also reflected in the UV–Vis absorption spectra as shown in Fig. 2. Upon addition of F4-TCNQ, new bands/peaks at longer wavelengths appear in the solution mixture as compared to the spectra of their pure solutions. In the **4a** and **4b** absorption spectra, there are no absorption above 700 nm, while the mixture of F4-TCNQ with **4a** and **4b** show additional strong absorption peaks around 760 and 870 nm, which are attributed to the absorption of anion radical of F4-TCNQ [20]. Concomitantly, the absorption intensity of F4-TCNQ decreases dramatically

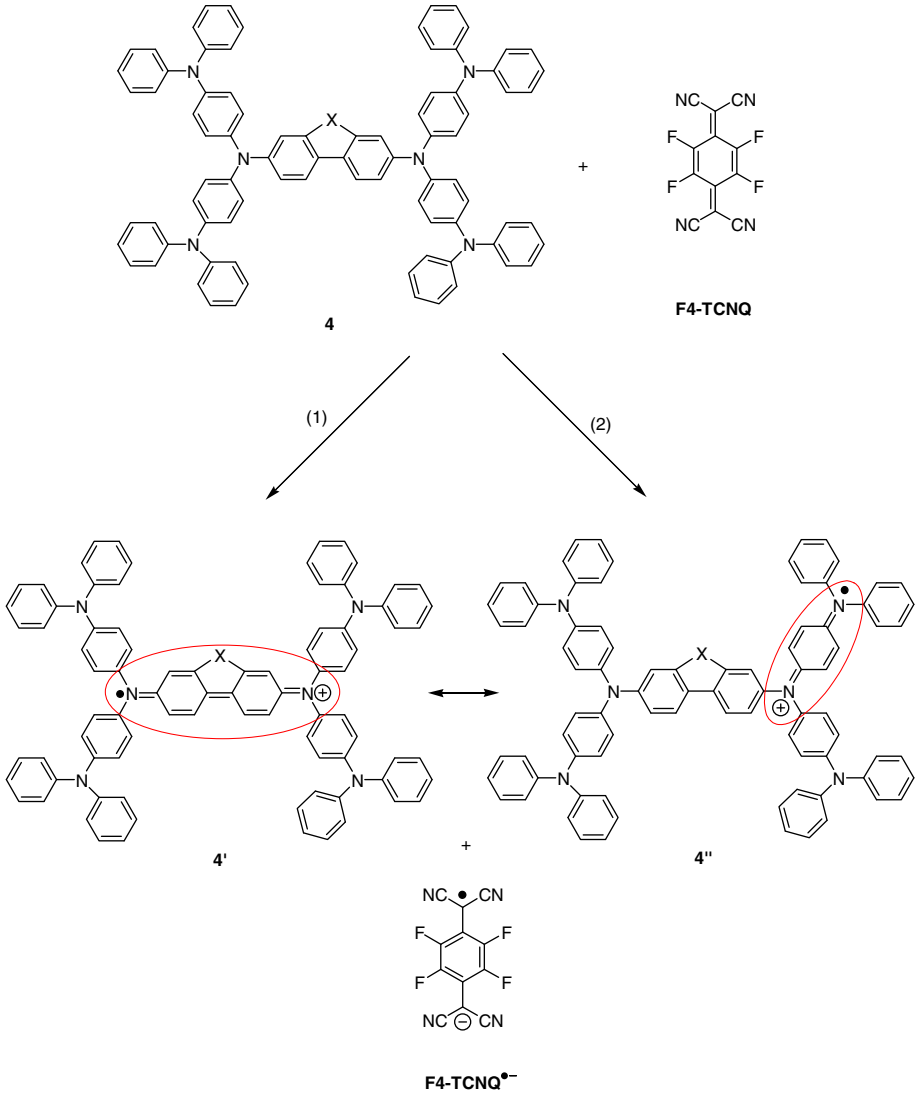

Fig. 1. Possible reaction mechanism for electron-donor **4** and electron-acceptor F4-TCNQ.

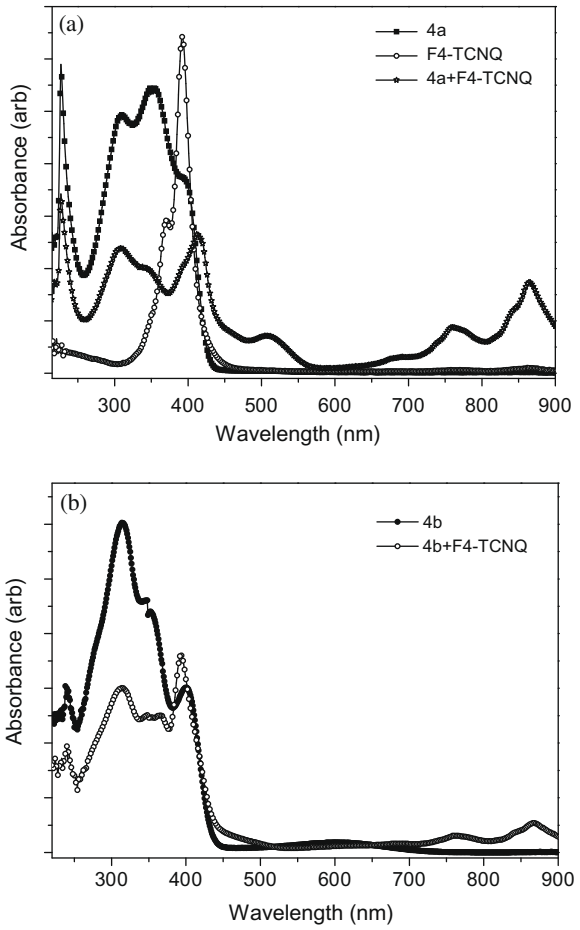

Fig. 2. (a) UV–Vis absorption of **4a** (10^{-5} M), F4-TCNQ (10^{-5} M) and **4a** (10^{-5} M) + F4-TCNQ (10^{-5} M) in DCM and (b) UV–Vis absorption of **4b** (10^{-5} M) and **4b** (10^{-5} M) + F4-TCNQ (10^{-5} M) in DCM.

in the solution mixture. This illustrates that the charge transfer (CT) complex is formed between **4a** (and **4b**) and F4-TCNQ which also implies that these materials doped with F4-TCNQ would form a good *p*-type system. In addition, the charge transfer band of F4-TCNQ doped **4a** system was about 10 times higher than that of F4-TCNQ doped **4b** system, suggesting a more efficient charge transfer between F4-TCNQ and **4a** than F4-TCNQ and **4b**. This may explain the better hole conduction in the **4a** doped with F4-TCNQ thin-film shown in the next section.

2.3. p-Type doping properties in thin-films

From a chemical point of view, in amorphous thin-films, the *p*-type doping of a hole transporting molecules *D* by electron-acceptor molecules *A* is determined by a mass action law (In this case, *D* concentration is much higher than *A* concentration):

$$D + \hat{D}A \rightleftharpoons D + [\hat{D}^{+}A^{-}] \rightleftharpoons D^{+} + \hat{D}A^{-} \tag{3}$$

Here, *D* is a random matrix molecule and $\hat{D}$ is the matrix molecule adjacent to the electron-acceptor, which is supposed to give the electron to the acceptor in the initial charge transfer step, this is exactly the reaction shown in Fig. 1 and Eq. (1). Thus, the intermediate state $[\hat{D}^{+}A^{-}]$ is a local charge transfer state, where the charges may be bound by different interactions and form a kind of complex. The final state is assumed to be unbound, i.e. the matrix molecule that carries the positive charge is so far away from the ionized acceptor that it does not feel the Coulomb interaction. In such a situation, the positive charge can move by hopping and the density of D^{+} can be associated with the hole density *p*. If a very strong electron-acceptor is used and the initial charge transfer (first step of reaction (3)) is complete, the hole density will be governed by the second step of reaction (3). The problem of the generation of free carriers is not only about the Coulomb attraction between two molecules with opposite charge. It is about the difference in the total energy between the following two states: (a) a matrix with a certain density of charged acceptors with holes bound to the acceptors and (b) the same matrix with mobile holes. Here, all kind of structural relaxation and quantum chemical reorganization processes have to be considered [21]. In our case, it could be thought or assumed that the F4-TCNQ acceptors could react with the host molecules in a great extent or even completely because of the energetically favorable reaction and the small electron-acceptor concentration. Therefore, the free hole density in the doping system shall be only controlled by the dissociation of the intermediate state $[\hat{D}^{+}A^{-}]$. In other words, besides the high tendency for electron transfer from electron-donor to electron-acceptor, another important factor that influences the conductivity of the doped system is the status of the intermediate $[\hat{D}^{+}A^{-}]$: the easier the dissociation, the higher conductivity is the doped system.

In order to study the hole transporting properties of **4a** and **4b** without or with doping, we fabricated hole-only devices with the structure of ITO/**4a** and **4b** with 0% or 1.5% F4-TCNQ (60 nm)/NPB (10 nm)/Al (where NPB = N,N′-bis-(1-naphthyl)-N,N′-dipheny-1,1′- biphenyl-4,4′-diamine). *N*,*N*′-bis-(1-naphthyl)-N,N′-dipheny-1,1′-biphenyl-4,4′-diamine). For comparison, the 2T-NATA hole-only devices with and without F4-TCNQ were fabricated simultaneously. The *I–V* measurements were carried out on these devices and the results are shown in Fig. 3. It is clearly indicated that the F4-TCNQ doped films of **4a**, **4b** and 2T-NATA exhibit significantly higher current as compared to their undoped counterparts, demonstrating high conductivity in the doped films. In the F4-TCNQ doped systems, **4a**-based film shows a greater improvement in conductivity with about 2–3 orders of magnitude increase in hole current with respect to the undoped film. It is important to note that the current densities of F4-TCNQ doped **4a**, **4b,** and 2T-NATA hole-only devices at 3 V are 135, 6.6 and 51.8 mA/cm^2, respectively. These findings are consistent with the HOMO data determined which indicate that the HOMO level of **4a** is lower than that of **4b** and 2T-NATA, as shown in Table 1. In addition, the absorption spectra in the doping system indicate that the degree of charge transfer in **4a**/F4-TCNQ system is higher than that of **4b**/F4-TCNQ system due to the lower HOMO of **4a**. Therefore, F4-TCNQ doped **4a** film showed higher hole conductivity than those of F4-TCNQ doped **4b** and 2T-NATA

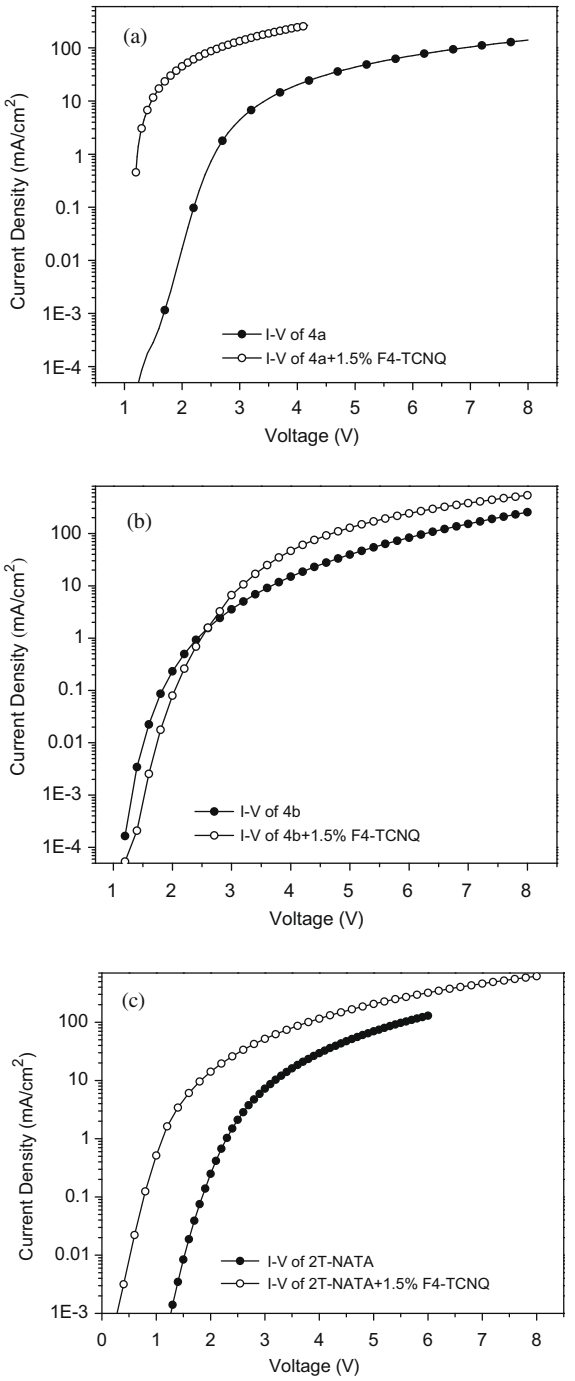

Fig. 3. I–V characteristics of (a) **4a**, (b) **4b,** and (c) 2T-NATA hole-only devices with and without F4-TCNQ.

films. As a result, **4a** is anticipated to be a better candidate for the *p*-type doping host material than 2T-NATA.

2.4. Application in OLED devices

Encapsulated OLED devices with a sheet desiccant inside a glass cover were fabricated using F4-TCNQ doped **4a** and **4b** as a HIL. The device structure is ITO/**4a** or **4b**:1.5% F4-TCNQ (150 nm)/NPB (10 nm)/Alq_3 (60 nm)/LiF (1 nm)/Al. The performance of the devices was tested and the *I–V–B* characteristics are shown in Table 2 and Fig. 4. The operation lifetimes were measured at a constant current of 20 mA/cm^2. The lifetime was recorded after a 10-h burn-in. For comparison, the OLED using 2T-NATA doped with F4-TCNQ as a HIL was also fabricated and tested under the same conditions. The results are summarized in Table 2.

Due to the doping of HIL, a high luminance is achieved at low voltage which results in a high power efficiency even though a comparatively thick HTL (160 nm in thickness) is used. For the **4a**-based device, the turn-on voltage, defined as the bias at a brightness of 1 cd/m^2, is only 2.7 V. At 20 mA/cm^2, the device driving voltage is 6.0 V and current efficiency is 5.2 cd/A as compared to the commonly used 2T-NATA doped with F4-TCNQ as a HIL, the driving voltage is 6.7 V with a current efficiency of 4.5 cd/A at the same current density. These results indicate that **4a** is a superior material for the HIL in OLED. For **4b**-based device, it shows a slightly higher driving voltage which agrees with its relatively inferior hole transporting properties in F4-TCNQ doped thin-film and a shorter lifetime. Fig. 5 shows the stability curve of **4a**-based device to its half brightness. As shown in the figure that such an OLED device has an operation lifetime of 1500 h at 20 mA/cm^2, and the driving voltage increasing is about 0.7 mV/h. This result demonstrates that our material **4a** is a very useful and stable *p*-type dopant host for the use of OLEDs and has a great potential for practical applications.

3. Experimental

3.1. Synthesis

2a. A mixture of 2,7-dibromo-9,9-bis(*n*-butyl)fluorene, **1a** (4.36 g, 10.0 mmol), diphenylamine (3.72 g, 22.0 mmol), palladium(II) acetate (0.11 g, 0.5 mmol), tri-(*o*-tolyl)phosphine (0.30 g, 1.0 mmol) and sodium *tert*-butoxide (2.88 g, 30.0 mmol) in dry toluene (50 mL) was stirred under a nitrogen atmosphere at 110 °C for 24 h. After cooling to room temperature, the reaction mixture was poured into a saturated aqueous solution of ammonium chloride and extracted with dichloromethane (3 × 60 mL). The combined organic extract was washed with water and dried over anhydrous Na_2SO_4. Evaporation of volatiles gave a brown solid, which was separated by silica gel column chromatography using petroleum ether/dichloromethane as a gradient eluent affording **2a** in 72% yield (4.4 g) as a white solid. ^{1}H NMR (400 MHz, $CDCl_3$, δ) 7.47 (d, J = 8.0 Hz, 2H), 7.22–7.25 (m, 8H), 7.07–7.13 (m, 10H), 6.97–7.01 (m, 6H), 1.73–1.77 (m, 4H), 1.02–1.10 (m, 4H), 0.72 (t, J = 7.6 Hz, 6H), 0.64–0.67 (m, 4H). ^{13}C NMR (100 MHz, $CDCl_3$, δ) 152.0, 148.0, 146.4, 136.2, 129.1, 123.7, 123.6, 122.3, 119.7, 119.4, 54.9, 39.7, 26.1, 22.9, 13.9. MS (MALDI-TOF) m/z 612.8 (M^+).

2b. The synthetic procedure for **2a** was followed using 2,7-dibromofluorenone, **1b** (3.38 g, 10.0 mmol), Ph_2NH (3.72 g, 22.0 mmol), *t*-BuONa (2.88 g, 30.0 mmol), $Pd(OAc)_2$

Table 2
Summaries of OLED Performance.

Device[a]	HIL	Turn On/V[b]	V_{20}/V	CE_{20}/cd/A[c]	$Lifetime_{20}$/h[d]
I	2T-NATA	2.7	6.7	4.5	1600
II	**4a**	2.7	6.0	5.2	1500
III	**4b**	3.1	7.6	3.4	1100

[a] Device I: ITO/2T-NATA:1.5%F4-TCNQ(150 nm)/NPB(10 nm)/Alq_3(60 nm)/LiF(1 nm)/Al. Device II: ITO/**4a**:1.5%F4-TCNQ(150 nm)/NPB(10 nm)/Alq_3(60 nm)/LiF(1 nm)/Al. Device III: ITO/**4b**:1.5%F4-TCNQ(150 nm)/NPB(10 nm)/Alq_3(60 nm)/LiF(1 nm)/Al.
[b] Turn on is the voltage to show 1 cd/m^2 luminance.
[c] CE_{20} refers to the current efficiency under 20 mA/cm.
[d] $Lifetime_{20}$ presents the lifetime at constant driven-current of 20 mA cm.

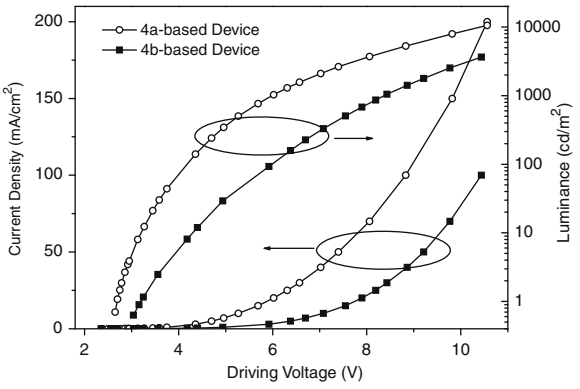

Fig. 4. I–V–B characteristic of **4a**- and **4b**-based OLED devices.

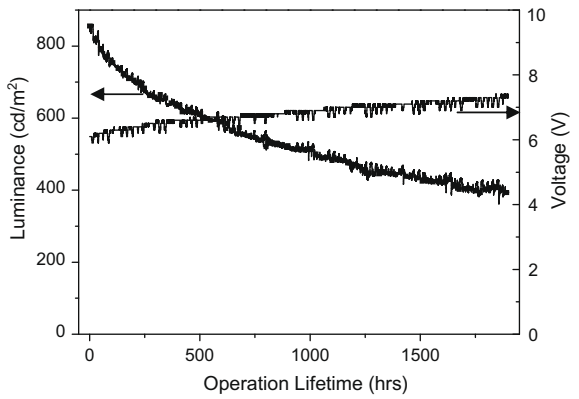

Fig. 5. Operation lifetime of **4a**-based OLED device.

(0.11 g, 0.5 mmol), P(*o*-tolyl)$_3$, (0.30 g, 1.0 mmol) and dry toluene (50 mL). The product was purified by silica gel column chromatography using petroleum ether/dichloromethane as a gradient eluent affording 3.48 g (68%) of **2b** as a dark red solid. ^{1}H NMR (400 MHz, $CDCl_3$, δ) 7.24 (d, J = 2.0 Hz, 2H), 7.14–7.19 (m, 10H), 6.94–7.04 (m, 14H). ^{13}C NMR (100 MHz, $CDCl_3$, δ) 193.3, 148.1, 147.0, 137.9, 135.7, 129.4, 128.5, 124.5, 123.4, 120.3, 119.3. HRMS (MALDI-TOF) Calc. for $C_{37}H_{26}N_2O$: 514.2040. Found: 514.2041.

3a. A mixture of **2a** (4.28 g, 7.0 mmol) and NBS (5.0 g, 28.0 mmol) in 50 mL of $CHCl_3$ were stirred at room temperature for 4 h. Evaporation of solvent under vacuum resulted in a yellow solid that was adsorbed on silica gel and purified by flash column chromatography using dichloromethane/petroleum ether mixture as eluent affording **3a** in 97% yield (6.30 g) as a white solid. ^{1}H NMR (400 MHz, $CDCl_3$, δ) 7.49 (d, J = 8.0 Hz, 2H), 7.34 (d, J = 8.8 Hz, 8H), 7.02 (d, J = 2.0 Hz, 2H), 6.97 (m, 10H), 1.75–1.79 (m, 4H), 1.02–1.10 (m, 4H), 0.72 (t, J = 7.2 Hz, 6H), 0.61–0.69 (m, 4H). ^{13}C NMR (100 MHz, $CDCl_3$, δ) 152.3, 146.6, 145.6, 136.6, 132.2, 125.1, 123.6, 120.1, 119.3, 115.2, 55.0, 39.6, 26.1, 22.9, 14.0. MS (MALDI-TOF) m/z 928.1 (M^+).

3b. The above procedure for **3a** was followed using **2b** (3.4 g, 6.6 mmol) and NBS (4.71 g, 26.5 mmol). The crude product was purified by silica gel flash column chromatography using dichloromethane/petroleum ether mixture as eluent affording **3b** in 92% yield (5.04 g) as a dark purple solid. ^{1}H NMR (400 MHz, $CDCl_3$, δ) 7.37 (d, J = 8.8 Hz, 8H), 7.28–7.30 (m, 4H), 7.11 (dd, J = 2.0, 8.0 Hz, 4H), 6.94 (d, J = 8.8 Hz, 8H). ^{13}C NMR (100 MHz, $CDCl_3$, δ) 192.7, 147.4, 145.6, 138.6, 135.8, 132.6, 129.0, 125.8, 120.8, 119.6, 116.4. MS (MALDI-TOF) m/z 829.9 (M^+).

4a. A dried 250 mL two-necked flask containing the solution of **3a** (4.64 g, 5.0 mmol), Ph_2NH (4.06 g, 24.0 mmol), *t*-BuONa (2.88 g, 30.0 mmol), $Pd(dba)_2$ (116 mg, 0.2 mmol), tri-*tert*-butylphosphine (40 mg, 0.2 mmol) and 70 mL of dry toluene was heated at 90 °C overnight with good stirring under N_2. After cooling to room temperature, the purple-blue mixture was poured into a saturated aqueous solution of ammonium chloride and extracted twice with toluene. The combined organic layers were washed with brine, dried over anhydrous magnesium sulfate and evaporated under vacuum. The residue was rapidly eluted through silica gel column using toluene/hexane (4:1) to give crude product, which was further purified by crystallization from EtOAc/EtOH affording 5.44 g (85% yield) of **4a** as a light-yellow solid. ^{1}H NMR (400 MHz, C_6D_6, δ) 7.35–7.38 (m, 4H), 7.21 (dd, J = 1.6, 8.0 Hz, 2H), 7.12–7.16 (m, 24H), 7.00–7.08 (m, 24H), 6.83 (t, J = 7.6 Hz, 8H), 1.70–1.73 (m, 4H), 0.94–1.07 (m, 4H), 0.84–0.91 (m, 4H), 0.63 (t, J = 7.6 Hz, 6H) ^{13}C NMR (100 MHz, C_6D_6, δ) 152.5, 148.4, 147.1, 143.7, 143.0, 136.5, 129.5, 125.9, 125.0, 124.2, 123.7, 122.7, 120.4, 119.4, 55.2, 40.0, 26.5, 23.2, 14.1. HRMS (MALDI-TOF) calc. for $C_{93}H_{80}N_6$: 1281.6471. Found: 1281.6514, Anal. Calc. for $C_{93}H_{80}N_6$: C 87.15, H 6.29, N 6.56. Found: C 87.30, H 6.19, N 6.40.

4b. The general amination procedure was followed using **3b** (2.1 g, 2.53 mmol), Ph_2NH (2.06 g, 12.2 mmol),

$Pd(dba)_2$ (58.7 mg, 0.1 mmol), P(*t*-Bu)$_3$ (20.2 mg, 0.1 mmol), *t*-BuONa (1.46 g, 15.2 mmol) and toluene. The crude product was purified by silica gel flash column chromatography (toluene/hexane) and then by crystallization from THF/CH_3OH affording 2.03 g (68% yield) of **4b** as a red solid. ^{1}H NMR (400 MHz, C_6D_6, δ) 7.68 (d, J = 2.0 Hz, 2H), 7.09–7.13 (m, 18H), 7.02–7.06 (m, 16H), 6.93–6.98 (m, 16H), 6.89 (d, J = 8.0 Hz, 2H), 6.83 (t, J = 7.2 Hz, 8H). ^{13}C NMR (100 MHz, C_6D_6, δ) 192.7, 148.6, 148.2, 144.0, 142.2, 137.9, 136.4, 129.6, 127.6, 125.9, 125.5, 124.5, 123.0, 120.6, 118.6. HRMS (MALDI-TOF) calc. for $C_{85}H_{62}N_6O$: 1182.4980; Found: 1182.4988. Anal. Calc. for $C_{85}H_{62}N_6O$: C 86.27, H 5.28, N 7.10; found: C 86.14, H 5.17, N 7.02.

3.2. Device fabrication

OLED and hole-only devices were fabricated using a vacuum thermal evaporation chamber with a base pressure of 1×10^{-6} Torr. All the materials were deposited in one pump-down. Two shadow masks were used to define the deposition areas for organic and metal cathode, respectively. The *I–V* characteristics of hole-only devices were measured with a computer-controlled DC power supply at room temperature in open air. OLED devices were encapsulated with sheet desiccant under dry N_2 atmosphere before measurements. The luminance of OLEDs was measured with PR650 spectrophotometer and a KETHLEY 236 source meter. The lifetime of OLED device was recorded by a homemade lifetime measurement system at constant current mode. The ionization potential (or HOMO) of a thin-film was measured by ultraviolet photoemission spectroscopy using Surface Analyzer model AC-2.

4. Conclusions

In summary, we have designed and synthesized two new *p*-phenylenediamine-substituted fluorenes, **4a** and **4b** which possess a high glass transition temperature and a good hole transport ability. The *p*-type doping properties of these materials were studied using F4-TCNQ as a *p*-type dopant in hole-only device. Furthermore, the mechanism in the doping system was discussed and some insights were highlighted. The OLED device with a HIL utilizing **4a**/**4b** doped with F4-TCNQ were fabricated and characterized. The pure Alq_3-based device using **4a** doped with F4-TCNQ as a HIL shows an operation lifetime of 1500 h at 20 mA/cm^2, and the driving voltage increasing about 0.7 mV/h. These results suggest that **4a** is a useful and stable hole injection material for OLEDs which shows a great potential for practical applications.

Acknowledgements

This work is supported by Guangdong-HK ITF (GHP/057/05), Research Grants Council of Hong Kong, Earmarked Research Grant HKBU 202507, Nanjing University of Posts and Telecommunications Grant NY207162 and Natural Science Foundation of Jiangsu High Education under Grant 08KJB430011.

References

[1] C.D. Dimitrakopoulos, P.R.L. Malenfant, Adv. Mater. 14 (2002) 99.
[2] (a) P. Peumans, A. Yakimov, S.R. Forrest, J. Appl. Phys. 93 (2003) 3693;
(b) S. Günes, H. Neugebauer, N.S. Saricifitci, Chem. Rev. 107 (2007) 1324.
[3] (a) T.P.I. Saragi, T. Spehr, A. Siebert, T. Fuhrmann-Lieker, J. Salbeck, Chem. Rev. 17 (2007) 1011;
(b) A. Gadisa, W. Mammo, L.M. Andersson, S. Admassie, F. Zhang, M.R. Andersson, O. Inganas, Adv. Func. Mater. 17 (2007) 3836.
[4] (a) C.K. Chan, E.-G. Kim, J.-L. Bredas, A. Kahn, Adv. Funct. Mater. 16 (2006) 831;
(b) Z.Q. Gao, B.X. Mi, G.Z. Xu, Y.Q. Wan, M.L. Gong, K.W. Cheah, C.H. Chen, Chem. Commun. (2008) 117.
[5] M. Pfeiffer, K. Leo, X. Zhou, J.S. Huang, M. Hofmann, A. Werner, J. Blochwitz-Nimoth, Org. Electron. 4 (2003) 89.
[6] K. Walzer, B. Maenning, M. Pfeiffer, K. Leo, Chem. Rev. 107 (2007) 1233.
[7] (a) J.S. Huang, M. Pfeiffer, A. Werner, J. Blochwitz, K. Leo, S. Liu, Appl. Phys. Lett. 80 (2002) 139;
(b) G. He, M. Pfeiffer, K. Leo, Appl. Phys. Lett. 85 (2004) 3911.
[8] B. Maennig, J. Drechsel, D. Gebeyehu, P. Simon, F. Kozlowski, A. Werner, F. Li, S. Grundmann, S. Sonntag, M. Koch, K. Leo, M. Pfeiffer, H. Hoppe, D. Meissner, N.S. Sariciftci, I. Riedel, V. Dyakonov, J. Parisi, Appl. Phys. A 79 (2004) 1.
[9] X. Zhou, M. Pfeiffer, J. Blochwitz, A. Werner, A. Nollau, T. Fritz, K. Leo, Appl. Phys. Lett. 78 (2001) 410.
[10] G. Schwartz, M. Pfeiffer, S. Reineke, K. Walzer, K. Leo, Adv. Mater. 19 (2007) 3672.
[11] R. Meerheim, K. Walzer, M. Pfeiffer, K. Keo, Appl. Phys. Lett. 89 (2006) 061111.
[12] X. Zhou, J. Blochwitz, M. Pfeiffer, A. Nollau, T. Fritz, K. Leo, Adv. Funct. Mater. 11 (2001) 310.
[13] P. Chen, G. Yang, T. Liu, T. Li, M. Wang, W. Huang, Polym. Int. 55 (2006) 473.
[14] (a) K.-F. Shao, Y.-F. Li, L.-M. Yang, X.-J. Xu, G. Yu, Y.-Q. Liu, Chem. Lett. 34 (2005) 1604;
(b) Z.H. Li, M.S. Wong, H. Fukutani, Y. Tao, Chem. Mater. 17 (2005) 5032.
[15] (a) L. Oldridge, M. Kastler, K. Müllen, Chem. Commun. (2006) 885;
(b) Z.H. Li, M.S. Wong, Y. Tao, H. Fukutani, Org. Lett. 9 (2007) 3659.
[16] (a) Z.H. Li, M.S. Wong, Y. Tao, J.P. Lu, Chem. Eur. J. 11 (2005) 3285;
(b) Z.Q. Gao, Z.H. Li, P.F. Xia, M.S. Wong, K.W. Cheah, C.H. Chen, Adv. Funct. Mater. 17 (2007) 3194;
(c) T.-C. Chao, Y.-T. Lin, C.-Y. Yang, T.S. Hung, H.-C. Chou, C.-C. Wu, K.-T. Wong, Adv. Mater. 17 (2005) 992;
(d) P.A. Levermore, R. Xia, W. Lai, X.H. Wang, W. Huang, D.D.C. Bradley, J. Phys. D: Appl. Phys. 40 (2007) 1896.
[17] Y. Shirota, H. Kageyama, Chem. Rev. 107 (2007) 953.
[18] R.C. Wheland, J. Am. Chem. Soc. 98 (1976) 3926.
[19] Notes: At Ref [4b], the first reduction potential of F4-TCNQ was measured as 0.61 V vs. Ag/AgCl electrode in saturated KCl solution, where the potential of reference electrode itself is 0.200 V. According to the SCE potential of 0.242, the first reduction potential of F4-TCNQ vs. SCE is calculated as: 0.61 + 0.200 – 0.242 = 0.568 V.
[20] L.R. Melby, R.J. Harder, W.R. Hertlbr, W. Mahler, R.E. Benson, W.E. Mochel, J. Am. Chem. Soc. 84 (1962) 3374.
[21] B. Kramer (Ed.), Advances in Solid State Physics, vol. 39, Vieweg, Braunchweig, Wiesbaden, 1999, pp. 77–90.